



# CHORUS

This is the accepted manuscript made available via CHORUS. The article has been published as:

## Optimal Bandwidth for High Efficiency Thermoelectrics

Jun Zhou, Ronggui Yang, Gang Chen, and Mildred S. Dresselhaus

Phys. Rev. Lett. **107**, 226601 — Published 22 November 2011

DOI: [10.1103/PhysRevLett.107.226601](https://doi.org/10.1103/PhysRevLett.107.226601)

# Optimal Band Width for High Efficiency Thermoelectrics

Jun Zhou<sup>1</sup> and Ronggui Yang<sup>1</sup>

<sup>1</sup>Department of Mechanical Engineering

University of Colorado, Boulder, CO 80309, USA

Gang Chen<sup>2</sup> and Mildred S. Dresselhaus<sup>3</sup>

<sup>2</sup>Department of Mechanical Engineering and <sup>3</sup>Department of Physics

Massachusetts Institute of Technology, Cambridge, MA 02139, USA

## ABSTRACT

The thermoelectric figure of merit ( $ZT$ ) in narrow conduction bands of different material dimensionalities, with a bandwidth of several  $k_B T$ , is investigated for different carrier scattering models. When the bandwidth is close to zero, the transport distribution function is indeed finite, not infinite as previously speculated by Mahan and Sofo [Proc. Natl. Acad. Sci. USA **93**, 7436 (1996)], even though the carrier density of states goes to infinity. Such a finite transport distribution function results in zero electrical conductivity and thus zero power factor and zero  $ZT$ . We point out that the optimal  $ZT$  cannot be found in an extremely narrow conduction band. The existence of an optimal bandwidth for maximum  $ZT$  depends strongly on the scattering mechanisms and the dimensionality of the material. A nonzero optimal bandwidth for maximizing  $ZT$  is also dependent on a dimensionless parameter which is proportional to the lattice thermal conductivity. Larger maximum  $ZT$  can be obtained for materials with smaller lattice thermal conductivity. Our results could provide a useful guide for searching for high efficiency thermoelectric materials.

KEYWORDS: thermoelectrics, band structure, carrier relaxation time, thermal conductivity

PACS numbers: 72.10.-d, 71.20.-b, 72.20.Pa

Recently, there has been an increasing interest in using thermoelectrics (TE) for

solar-thermal applications, waste heat recovery and thermal management of electronics [1,2,3]. The efficiency of a solid-state TE device for power generation and electronic refrigeration is determined by the figure of merit ( $ZT$ ) of the material [4]:

$$ZT = \frac{\sigma S^2}{\kappa_e + \kappa_p} T, \quad (1)$$

where  $\sigma$  is the electrical conductivity,  $S$  is the Seebeck coefficient,  $\kappa_e$  is the electronic thermal conductivity,  $\kappa_p$  is the lattice thermal conductivity, and  $T$  is the absolute temperature. Searching for high  $ZT$  materials is essential in TE power generation and refrigeration. One way to increase  $ZT$  is to reduce  $\kappa_p$  without significantly changing the electronic transport properties [5,6,7,8]. Another way is to maximize the power factor for a given  $\kappa_p$  through optimizing the electronic band structure of the material. The original theoretical work by Mahan and Sofo [9] showed that an electronic structure with a delta-shaped transport distribution function (TDF) leads to a maximum  $ZT$ . Many of the band structure engineering works for TE materials over the past decade have somewhat followed this guideline by introducing a sharp density of states (DOS) [10,11,12,13,14], including the search for rare-earth compounds and transition-metal compounds [15,16,17], introducing impurity levels in bulk semiconductor materials [18], and the nanostructured materials with low-dimensional miniband formation [1,19].

Though mathematically rigorous, Mahan and Sofo also noted in their original paper [9] that the exact delta-shaped TDF cannot be found in real materials due to the energy-dependent relaxation time and carrier velocity. It is therefore very meaningful to re-investigate what is the best electronic structure of materials to maximize  $ZT$  when scattering physics of carriers is considered. In this letter, we study TE transport properties in a

narrow conduction band with a bandwidth on the order of  $k_B T$ , where  $k_B$  is the Boltzmann constant, for different scattering models in different dimensionalities of the material.

Without losing the generality, we start our study using the nearest-neighbor tight-binding model in one-dimensional (1D), two-dimensional (2D), and three-dimensional (3D) systems with a lattice constant  $a$ . The lattice points of these generalized systems could be quantum dots (QDs), rare-earth atoms, or transition metal atoms. The quantum-confined electrons in QDs (or  $f$ -electrons in rare-earth elements,  $d$ -electrons in transition metal elements) could transport between the nearest-neighbor lattice points. Depending on the dimensionality, the dispersion relation  $E_\alpha(\mathbf{k})$  for these quantum-confined carriers can be written as:

$$E_{1D}(\mathbf{k}) = -2J_{1D} \cos k_x a, \quad (2a)$$

$$E_{2D}(\mathbf{k}) = -2J_{2D} (\cos k_x a + \cos k_y a), \quad (2b)$$

$$E_{3D}(\mathbf{k}) = -2J_{3D} (\cos k_x a + \cos k_y a + \cos k_z a), \quad (2c)$$

where the subscript for the dimensionality  $\alpha = 1D, 2D, \text{ and } 3D$  and  $\mathbf{k} = (k_x, k_y, k_z)$  is the wave vector of a carrier. Here, the bandwidths are  $W_{1D} = 4J_{1D}$ ,  $W_{2D} = 8J_{2D}$ , and  $W_{3D} = 12J_{3D}$ , where  $J_\alpha$  is the coupling constant which is usually on the order of a few meV. When the quantum-confinement potential goes to infinity, both the coupling constant and the bandwidth become zero for a fixed lattice constant.

By solving the linearized Boltzmann equations within the relaxation time approximation, the TE transport properties are related to the TDF  $\Xi_\alpha(E)$  as:

$$\sigma_\alpha = L_{\alpha,0}, \quad S_\alpha = \frac{L_{\alpha,1}}{TL_{\alpha,0}}, \quad \kappa_{\alpha,e} = \frac{1}{T} \left[ L_{\alpha,2} - \frac{L_{\alpha,1}^2}{L_{\alpha,0}} \right], \quad (3a)$$

$$L_{\alpha,i} = e^{2-i} \int_{-W_\alpha/2}^{W_\alpha/2} dE \Xi_\alpha(E) (E - \mu)^i \left( -\frac{\partial f_0}{\partial E} \right), \quad (3b)$$

where  $i = 0, 1, \text{ and } 2$ ,  $E$  is the energy of carriers,  $\mu$  is the chemical potential,  $e$  is the carrier charge, and  $f_0 = [e^{(E-\mu)/k_B T} + 1]^{-1}$  is the Fermi-Dirac distribution.  $\Xi_\alpha(E)$  is related to the band structure and the scattering physics as [9]:

$$\Xi_\alpha(E) = 2 \sum_{\mathbf{k}} v_{\alpha,x}^2(\mathbf{k}) \tau_\alpha(\mathbf{k}) \delta[E - E_\alpha(\mathbf{k})], \quad (4)$$

where  $v_{\alpha,x}(\mathbf{k}) = \frac{1}{\hbar} \frac{\partial E_\alpha(\mathbf{k})}{\partial k_x} = \frac{2J_\alpha a}{\hbar} \sin(k_x a)$ ,  $\tau_\alpha(\mathbf{k})$  is the relaxation time of carriers, the factor 2 comes from the spin degeneracy, and  $\hbar$  is the Planck constant.

We now consider the four different scattering models in common use for the carrier relaxation time where an isotropic one  $\tau_\alpha(\mathbf{k}) = \tau_\alpha(E_\alpha(\mathbf{k}))$  is assumed. We note that the results for other scattering models beyond these four models, such as  $\tau_\alpha(E) \sim E^{3/2}, E^{1/2}$ , and  $E^{-1/2}$ , could also be obtained similarly. The calculated TDF  $\Xi_\alpha(E)$  are shown in Table I: 1).  $\tau_\alpha(E)$  is inversely proportional to the broadening of the energy  $\Delta E$  which is about the bandwidth  $W_\alpha$  when  $\Delta E \ll k_B T$ , according to the uncertainty principle; 2). constant relaxation time  $\tau_\alpha(E) = \tau_{\alpha,0}$  which is widely used for TE transport property calculations [20]; 3).  $\tau_\alpha(E)$  is inversely proportional to the carrier DOS  $\tau_\alpha(E) = C_\alpha N_\alpha^{-1}(E)$ , where  $C_\alpha$  is a constant and the DOS is defined as  $N_\alpha(E) = 2 \sum_{\mathbf{k}} \delta[E - E_\alpha(\mathbf{k})] \propto 1/W_\alpha$ . This model has been often used for calculating the transport properties of rare-earth compounds [9]; and 4).  $\tau_\alpha(E)$  is proportional to a constant carrier mean free path (MFP)  $l_\alpha$ , i.e.,  $\tau_\alpha(E) = l_\alpha / v_\alpha(E)$ , which is widely used in narrow band conduction calculations [21,22]. Here  $v_\alpha(E) = v_\alpha(E_\alpha(\mathbf{k})) = \frac{1}{\hbar} |\nabla_{\mathbf{k}} E_\alpha(\mathbf{k})| \sim W_\alpha$ . Detailed derivations can be checked in Density of States and Transport Distribution Function [23].

Let us look at the case for an extremely narrow band first. When  $W_\alpha \rightarrow 0$ , the DOS is infinite since  $N_\alpha(E) \sim 1/W_\alpha$ . However, the TDF  $\Xi_\alpha(E)$  in Table I is always finite when

we consider different carrier scattering possibilities even though the DOS is infinite. This is very different from Mahan and Sofo's hypothesis [9] which assumes an infinite delta-shaped TDF. Such an infinite delta-shaped TDF can never hold in nature since it requires  $\tau_\alpha(E) \sim 1/W_\alpha^2$  [24], which cannot be found with known scattering models. Mathematically, for finite  $\Xi_\alpha(E)$ , all the transport coefficients  $\lim_{W_\alpha \rightarrow 0} L_{\alpha,i}$  in Eq. (3) must go to zero, which results in  $ZT_\alpha = 0$ . Only infinite  $\Xi_\alpha(E)$  can lead to nonzero  $\lim_{W_\alpha \rightarrow 0} L_{\alpha,i}$  because the integral limit in Eq. (3b) is from  $-W_\alpha/2$  to  $W_\alpha/2$ . In short, the TE power factor and ZT for an extremely narrow band is zero due to the finite TDF when the scattering mechanisms are considered explicitly rather than being optimized by a speculated infinite TDF [9].

After substituting the TDF  $\Xi_\alpha(E)$  shown in Table I into Eq. (3), the ZT expression in Eq. (1) can be re-written as:

$$ZT_\alpha = \frac{P_{\alpha,1}^2 / P_{\alpha,0}}{P_{\alpha,2} - P_{\alpha,1}^2 / P_{\alpha,0} + \gamma_\alpha}, \quad (5)$$

where the dimensionless integrals  $P_{\alpha,i}$  the dimensionless factors  $\gamma_\alpha$  strongly depend on the scattering physics.  $\gamma_\alpha$ , which is proportional to  $\kappa_p$ , is listed in Table II.  $P_{\alpha,i}$  can be written

out depending on the scattering physics.  $P_{\alpha,i} = \int_{-w_\alpha/2}^{w_\alpha/2} dx I_\alpha^{1/2}(\xi_\alpha) s(x)(x-b)^i$  for the

uncertainty principle and the constant relaxation time models,

$P_{\alpha,i} = \int_{-w_\alpha/2}^{w_\alpha/2} dx I_\alpha^{1/2}(\xi_\alpha) / I_\alpha^{-1/2}(\xi_\alpha) s(x)(x-b)^i$  for  $\tau \propto \text{DOS}^{-1}$ , and

$P_{\alpha,i} = \int_{-w_\alpha/2}^{w_\alpha/2} dx I_\alpha^0(\xi_\alpha) s(x)(x-b)^i$  for the constant carrier MFP model. We have rescaled all

the energy-related variables by  $k_B T$  for the above expressions with  $E = x k_B T$ ,  $W_\alpha = w_\alpha k_B T$ ,

$$\xi_\alpha = x / w_\alpha, \quad \mu = b k_B T, \quad \text{and} \quad s(x) = \frac{e^{x-b}}{(e^{x-b} + 1)^2}.$$

Physically, large ZT can be obtained with a small  $\gamma_\alpha$ , i.e., a low  $\kappa_p$ . This is consistent

with the efforts in the TE community trying to reduce  $\kappa_p$  through alloying and nanostructuring [1,7,8]. We first calculate the ZT with the constant carrier MFP scattering model. In our calculation, we make some simplifications to generalize the dimensionless factor  $\gamma_\alpha$  in order to compare ZTs between 1D, 2D and 3D systems. We assume all the carrier MFPs are the same, i.e.,  $l_{1D} = l_{2D} = l_{3D} = l_0$ , and  $\kappa_{p,1D} / a = \kappa_{p,2D} = \kappa_{p,3D} a = G$ , where  $G$  is the thermal conductance across each lattice point. Then  $\gamma_{1D} = \gamma_0 / 2$ ,  $\gamma_{2D} = \sqrt{2}\gamma_0$ , and  $\gamma_{3D} = 2\sqrt{3}\gamma_0$  where  $\gamma_0 = \frac{\hbar a G}{l_0 k_B^2 T}$ . Using typical values of  $a$  ( $\sim 0.5$ nm for  $d$ - or  $f$ -electrons, 1~5 nm for QDs) and  $l_0$  ( $\sim 10$ nm) and  $\kappa_p$  in good bulk TE materials is 0.2-3 W/mK [25], we estimate the value of  $\gamma_0$  to be 0.01~1 at room temperature.

Figures 1(a)-1(c) show the dependence of  $ZT_\alpha$  on the chemical potential  $\mu - W_\alpha / 2$ , where we choose the upper band edge ( $W_\alpha / 2$ ) as reference point, and the bandwidth  $W_\alpha$  when  $\gamma_0 = 0.06$  for the 1D, 2D and 3D systems. It should be pointed out that our model is valid only for narrow band conduction when the bandwidth is on the order of several  $k_B T$ . Therefore, we do not present the data for large bandwidths over  $10k_B T$  since the results would then be inaccurate. As expected, when the bandwidth  $W_\alpha \rightarrow 0$ ,  $ZT_\alpha$  goes to zero due to the finite TDF discussed above. In the 1D system, no obvious optimal point but an optimal ridge is found to maximize  $ZT_{1D}$  to be 6.4 when  $\mu - W_{1D} \sim 2k_B T$  and  $W_{1D} > 2.4k_B T$ . This is due to an energy-independent TDF  $\Xi_{1D} = 2l_0 / \pi\hbar$ . In this case, only the carriers which are close to the upper band edge (close to the chemical potential) contribute to the electronic transport. When the bandwidth increases, the contribution from this part changes very little for the energy-independent TDF and the carriers close to the lower band edge do not contribute to the transport. It is very different in the 2D and 3D systems since the TDF are

energy dependent. The maximum  $ZT_{2D}$  in Fig. 1(b) is found to be 3.5 with  $\mu - W_{2D}/2 \sim 1.5k_B T$  and the bandwidth  $W_{2D} \sim 3.5k_B T$  in the 2D system and the maximum  $ZT_{3D}$  to be 2.3 with  $\mu - W_{3D}/2 \sim k_B T$  and the bandwidth  $W_{3D} \sim 4.5k_B T$  in the 3D system. We find that the optimal bandwidth should be smaller for the lower dimensional materials and the maximum  $ZT$  is higher when both the carrier MFP and the thermal conductance  $G$  are assumed to be constants in different dimensionalities. We also compare the  $ZT_{3D}$  in the 3D system for different  $\gamma_0$  values in Figs. 1(c) and 1(d). We find that the maximum  $ZT_{3D}$  decreases from 2.4 to 1.6 and the corresponding optimal bandwidth shifts to a slightly higher value when  $\gamma_0$  changes from 0.06 to 0.1. From Figs. 1(c) and (d), we can see that it is essential to minimize the dimensionless factor  $\gamma_0$ , i.e., reduce  $\kappa_p$ , for high  $ZT_{3D}$  even if the electronic band structure is optimized. Now if we choose  $\kappa_{p,3D} = 0.2$  W/mK which is a rather small value for  $\kappa_p$  in semiconductors [25], one needs  $a^2/l_0 = 0.16$  nm at room temperature to make  $\gamma_0 = 0.06$ . If we further assume the carrier MFP  $l_0 = 10$  nm which is common in semiconductors, the lattice constant should be smaller than 1.3 nm.

Figures 2(a) and (b) show the dependence of the maximum  $ZT$  on the bandwidth with different  $\gamma_0$  values when  $\mu - W_{2D}/2$  is fixed to  $2k_B T$  in a 1D system and when  $\mu - W_{3D}/2$  is fixed to  $k_B T$  in a 3D system which are the optimal chemical potentials for the maximum  $ZT$  value we found from Fig. 1. In the 1D system, due to the energy independent TDF, we found that there is an individual optimal bandwidth to maximize  $ZT_{1D}$  for each  $\gamma_0$  only when  $\gamma_0 \leq 0.1$ . The optimal bandwidth increases with an increase of  $\gamma_0$ . When  $\gamma_0 > 0.1$ , the maximum  $ZT_{1D}$  does not depend on the bandwidth for  $W_{1D} > 3k_B T$ . In the 3D system, there always exists an optimal bandwidth for the maximum  $ZT_{3D}$  due to the

energy dependence of the TDF. The optimal bandwidth should be larger for larger  $\gamma_0$  (larger  $\kappa_p$ ). A larger  $\gamma_0$  also results in a lower maximum  $ZT_{3D}$ . To obtain a  $ZT_{3D}$  larger than 1 which is the value for current commercial TE materials, i.e.  $\text{Bi}_{2(1-x)}\text{Sb}_{2x}\text{Te}_3$  alloy [26] near room temperature,  $\gamma_0$  should be smaller than 0.14. At room temperature, the optimization requires  $\kappa_{p,3D} < 1 \text{ W/mK} \times \frac{l_0 \times 0.076 \text{ nm}}{a^2}$ . There have been a lot of attempts in reducing  $\kappa_p$  in 3D materials using nanostructuring approach to enhance  $ZT_{3D}$  [6,7,8]. This inequality for  $\kappa_{p,3D}$  essentially estimates the requirement on  $\kappa_p$  which makes  $ZT_{3D}$  over 1.

Figure 3 compares  $ZT_{3D}$  for the three different scattering models. In the calculation, we choose  $\tau_{3D,0} = 0.1 \text{ ps}$  for the constant relaxation time model,  $C_{3D} = 10^{34} \text{ s/Jm}^3$  which leads to an average relaxation time around 0.1 ps for the  $\tau \propto \text{DOS}^{-1}$  model, and  $l_{3D} = 10 \text{ nm}$  for the constant MFP model [27]. We also choose  $T = 300 \text{ K}$ ,  $\kappa_p = 0.2 \text{ W/mK}$ ,  $a = 1 \text{ nm}$ , and  $\mu - W_{3D}/2 = k_B T$ . We note that the uncertainty principle model is not valid when the bandwidth is larger than  $k_B T$ . We thus do not plot  $ZT_{3D}$  for the uncertainty model in this figure. Apparently, the optimal bandwidths for obtaining the maximum  $ZT_{3D}$  depend strongly on the relaxation time models. The optimal bandwidth for the maximum  $ZT_{3D}$  is found to be  $W_{3D} \sim 4k_B T$  for the constant MPF model with a maximum  $ZT_{3D} = 3.4$  and  $W_{3D} \sim 8k_B T$  for the constant relaxation time model with a maximum  $ZT_{3D} = 2.2$ . When  $\tau \propto \text{DOS}^{-1}$ ,  $ZT_{3D}$  always increases with the bandwidth  $W_{3D}$ . In Fig. 3, we further show the effect of an additional constant background TDF  $\Xi_{bg}$  to the TDF of narrow conduction band ( $\Xi_{3D}(E) \rightarrow \Xi_{3D}(E) + \Xi_{bg}$ ) for the constant MFP model. We find that zero  $ZT_{3D}$  remains when bandwidth is zero since the Seebeck coefficient is zero. The optimal bandwidth shifts to a lower value and the maximum  $ZT_{3D}$  would be smaller than 1 when  $\Xi_{bg} > 0.045\Xi_{3D}(0)$ .

In summary, we have calculated the thermoelectric figure of merit  $ZT$  by using the nearest-neighbor tight-binding model with different scattering physics for carrier relaxation time in 1D, 2D and 3D systems. When the bandwidth is close to zero, the transport distribution function is indeed finite, not infinite as previously speculated [9], even though the carrier density of states goes to infinity. Such a finite TDF results in zero electrical conductivity, power factor and  $ZT$ . We point out that the optimal  $ZT$  cannot be obtained in an extremely narrow conduction band. The existence of the optimal bandwidth for maximizing the  $ZT$  depends highly on the carrier scattering mechanisms. There exists an optimal bandwidth for a maximum  $ZT$  within the constant carrier MFP approximation or constant relaxation time approximation. If the carrier relaxation time is inversely proportional to DOS, no optimal bandwidth exists for achieving a maximum  $ZT$ . A nonzero optimal bandwidth for maximizing  $ZT$  is also dependent on a dimensionless parameter which is proportional to the lattice thermal conductivity. Our results could provide a useful guide for searching for high efficiency thermoelectric materials.

**Acknowledgements:** J.Z. and R.G.Y. acknowledge the support from DARPA (Contract N66001-10-C-4002), AFOSR (Grant No. FA9550-11-1-0109) and NSF (Grant No. CBET 0846561). G.C. and M.S.D. acknowledge support of the Solid State Solar-Thermal Energy Conversion Center (S3TEC), an Energy Frontier Research Center funded by the U.S. Department of Energy, Office of Science, Office of Basic Energy Sciences under Award Number: DE-SC0001299/DE-FG02-09ER46577.

Table I. TDF for the four scattering models: uncertainty principle; constant relaxation time; relaxation time inversely proportional to the DOS; and constant carrier MFP, where

$$\xi_\alpha = E/W_\alpha.$$

Scattering Model	$\tau_\alpha(E)$	$\Xi_{1D}(E)$	$\Xi_{2D}(E)$	$\Xi_{3D}(E)$
Uncertainty principle	$\hbar/W_\alpha$	$\frac{a}{\hbar} I_{1D}^{1/2}(\xi_{1D})$	$\frac{1}{4\hbar} I_{2D}^{1/2}(\xi_{2D})$	$\frac{1}{12\hbar a} I_{3D}^{1/2}(\xi_{3D})$
Constant $\tau$	$\tau_{\alpha,0}$	$\frac{W_{1D}\tau_{1D,0}a}{\hbar^2} I_{1D}^{1/2}(\xi_{1D})$	$\frac{W_{2D}\tau_{2D,0}}{4\hbar^2} I_{2D}^{1/2}(\xi_{2D})$	$\frac{W_{3D}\tau_{3D,0}}{12\hbar^2 a} I_{3D}^{1/2}(\xi_{3D})$
$\tau \propto \text{DOS}^{-1}$	$C_\alpha N_\alpha^{-1}(E)$	$C_{1D} \frac{W_{1D}^2 a^2}{4\hbar^2} \frac{I_{1D}^{1/2}(\xi_{1D})}{I_{1D}^{-1/2}(\xi_{1D})}$	$C_{2D} \frac{W_{2D}^2 a^2}{16\hbar^2} \frac{I_{2D}^{1/2}(\xi_{2D})}{I_{2D}^{-1/2}(\xi_{2D})}$	$C_{3D} \frac{W_{3D}^2 a^2}{36\hbar^2} \frac{I_{3D}^{1/2}(\xi_{3D})}{I_{3D}^{-1/2}(\xi_{3D})}$
Constant MFP	$l_\alpha/v_\alpha(E)$	$\frac{2l_{1D}}{\hbar} I_{1D}^0(\xi_{1D})$	$\frac{l_{2D}}{\sqrt{2}\hbar a} I_{2D}^0(\xi_{2D})$	$\frac{l_{3D}}{2\sqrt{3}\hbar a^2} I_{3D}^0(\xi_{3D})$

Table II. Dimensionless parameters  $\gamma_\alpha$  for different scattering models.

Scattering Model	$\gamma_{1D}$	$\gamma_{2D}$	$\gamma_{3D}$
Uncertainty principle	$\frac{\hbar k_{p,1D}}{ak_B^2 T}$	$\frac{4\hbar k_{p,2D}}{k_B^2 T}$	$\frac{12\hbar ak_{p,3D}}{k_B^2 T}$
Constant $\tau$	$\frac{\hbar^2 k_{p,1D}}{W_{1D} \tau_{1D,0} ak_B^2 T}$	$\frac{4\hbar^2 k_{p,2D}}{W_{2D} \tau_{2D,0} k_B^2 T}$	$\frac{12\hbar^2 ak_{p,3D}}{W_{3D} \tau_{3D,0} k_B^2 T}$
$\tau \propto \text{DOS}^{-1}$	$\frac{4\hbar^2 k_{p,1D}}{C_{1D} W_{1D}^2 a^2 k_B^2 T}$	$\frac{16\hbar^2 k_{p,2D}}{C_{2D} W_{2D}^2 a^2 k_B^2 T}$	$\frac{36\hbar^2 k_{p,3D}}{C_{3D} W_{3D}^2 a^2 k_B^2 T}$
Constant MFP	$\frac{\hbar k_{p,1D}}{2l_{1D} k_B^2 T}$	$\frac{\sqrt{2}\hbar ak_{p,2D}}{l_{2D} k_B^2 T}$	$\frac{2\sqrt{3}\hbar a^2 k_{p,3D}}{l_{3D} k_B^2 T}$

## Figure Captions

FIG. 1 (Color online)  $ZT$  plotted as functions of the chemical potential with respect to the upper band edge as reference  $\mu - W_\alpha/2$ , and of the bandwidth  $W_\alpha$  in (a) the 1D system when  $\gamma_0 = 0.06$ , (b) the 2D system when  $\gamma_0 = 0.06$ , (c) the 3D system when  $\gamma_0 = 0.06$ , and (d) the 3D system when  $\gamma_0 = 0.1$ .

FIG. 2 (Color online)  $ZT$  plotted as a function of the bandwidth  $W_\alpha$  in (a) the 1D system and (b) the 3D system when  $\gamma_0 = 0.06$ , 0.1, 0.14, and 0.18. The calculations use  $\mu - W_{1D}/2 = 2k_B T$  for the 1D and  $\mu - W_{3D}/2 = k_B T$  for the 3D system.

FIG. 3 (Color online)  $ZT_{3D}$  plotted as a function of the bandwidth  $W_{3D}$  in the 3D system for different carrier scattering models as shown in Table I: constant relaxation time  $\tau_{3D,0} = 0.1$  ps (solid curve); relaxation time inversely proportional to DOS where  $C_{3D} = 10^{34}$  s/Jm<sup>3</sup> (dashed curve); and constant carrier MFP  $l_{3D} = 10$  nm (dotted curve). The curve with square dots is the case when a constant background TDF  $\Xi_{bg} = 0.045 \Xi_{3D}(0)$  is superimposed to the narrow band TDF for the constant MFP model. The calculations use  $T = 300$  K,  $\kappa_p = 0.2$  W/mK,  $a = 1$  nm, and  $\mu - W_{3D}/2 = k_B T$ .

Figure 1

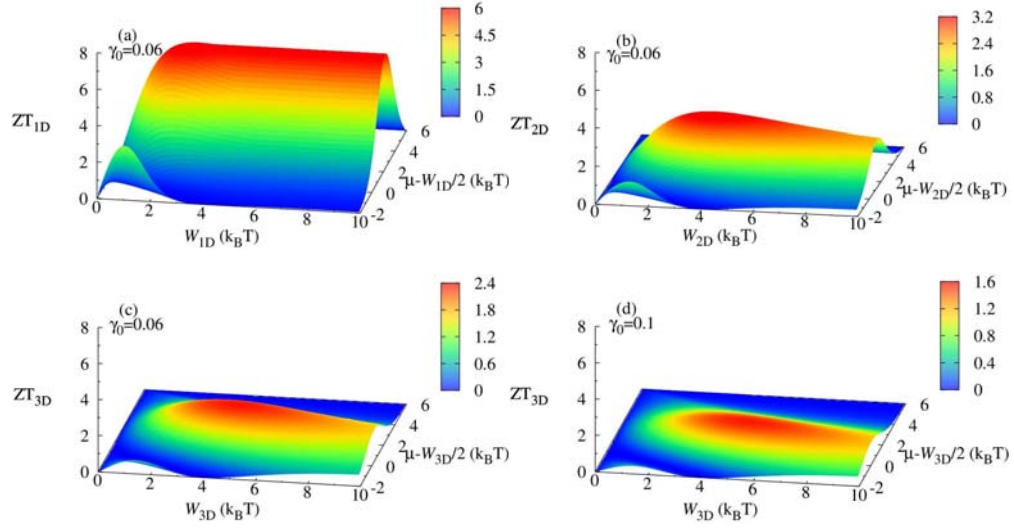


FIG. 1 (Color online)  $ZT$  plotted as functions of the chemical potential with respect to the upper band edge as reference  $\mu - W_\alpha/2$ , and of the bandwidth  $W_\alpha$  in (a) the 1D system when  $\gamma_0 = 0.06$ , (b) the 2D system when  $\gamma_0 = 0.06$ , (c) the 3D system when  $\gamma_0 = 0.06$ , and (d) the 3D system when  $\gamma_0 = 0.1$ .

Figure 2

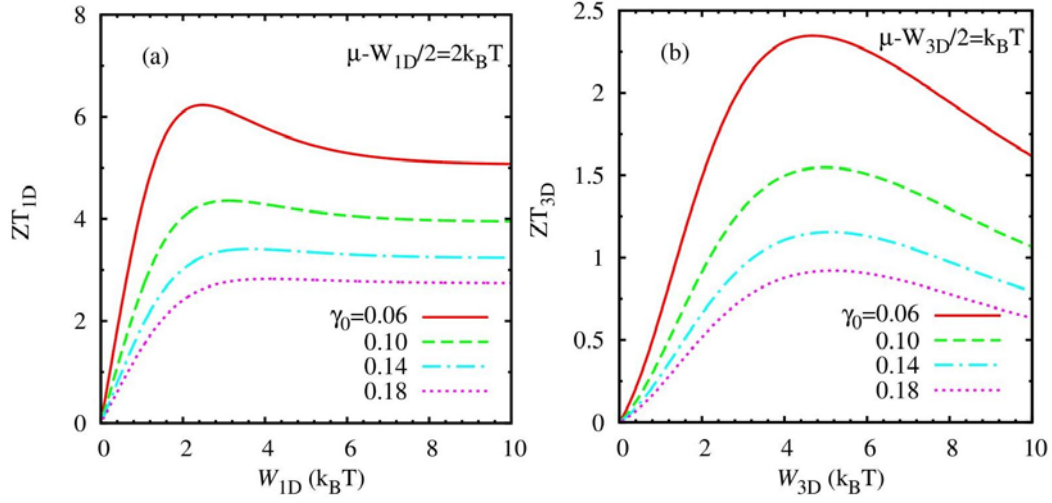


FIG. 2 (Color online)  $ZT$  plotted as a function of the bandwidth  $W_\alpha$  in (a) the 1D system and (b) the 3D system when  $\gamma_0 = 0.06$ , 0.1, 0.14, and 0.18. The calculations use  $\mu - W_{1D}/2 = 2k_B T$  for the 1D and  $\mu - W_{3D}/2 = k_B T$  for the 3D system.

Figure 3

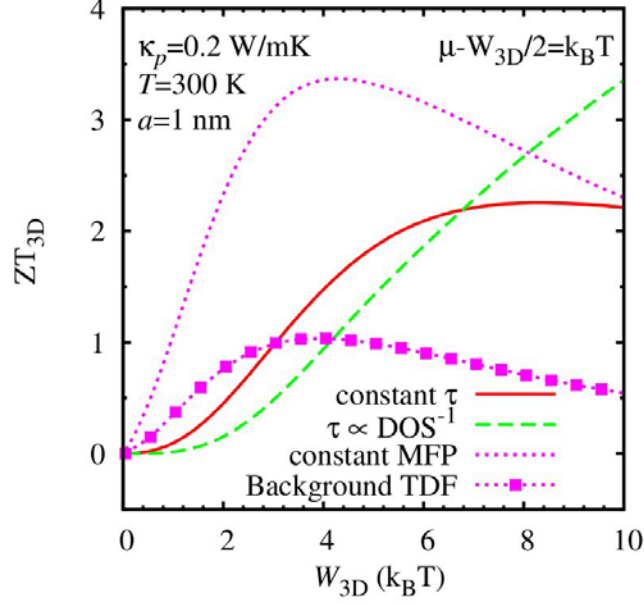


FIG. 3 (Color online)  $ZT_{3D}$  plotted as a function of the bandwidth  $W_{3D}$  in the 3D system for different carrier scattering models shown in Table I: constant relaxation time  $\tau_{3D,0} = 0.1$  ps (solid curve); relaxation time inversely proportional to DOS where  $C_{3D} = 10^{34}$  s/Jm<sup>3</sup> (dashed curve); and constant carrier MFP  $l_{3D} = 10$  nm (dotted curve). The curve with square dots is the case when a constant background TDF  $\Xi_{bg} = 0.045 \Xi_{3D}(0)$  is superimposed to the narrow band TDF for the constant MFP model. The calculations use  $T = 300$  K,  $\kappa_p = 0.2$  W/mK,  $a = 1$  nm, and  $\mu - W_{3D}/2 = k_B T$ .

## REFERENCES

- [1] M. S. Dresselhaus *et al.*, *Adv. Mater.* **19**, 1043 (2007).
- [2] L. E. Bell, *Science* **321**, 1457 (2008).
- [3] I. Chowdhury *et al.*, *Nature Nanotechnology* **4**, 235 (2009).
- [4] H. J. Goldsmid, *Electronic Refrigeration*, (Pion, London, 1986).
- [5] D. M. Rowe, in *Thermoelectric Handbook: Macro to Nano*, edited by D. M. Rowe (Taylor & Francis Group, Boca Raton, 2006), p. 1-9.
- [6] B. Poudel *et al.*, and Z. F. Ren, *Science* **320**, 634 (2008).
- [7] R. G. Yang and G. Chen, *Phys. Rev. B* **69**, 195316 (2004).
- [8] W. Kim *et al.*, *Phys. Rev. Lett.* **96**, 045901 (2006).
- [9] G. D. Mahan and J. Sofo, *Proc. Natl. Acad. Sci. USA* **93**, 7436 (1996).
- [10] D. Bilc *et al.*, *Phys. Rev. Lett.* **93**, 146403 (2004).
- [11] J. P. Heremans *et al.*, *Phys. Rev. Lett.* **88**, 216801 (2002).
- [12] S. Ahmad, K. Hoang, and S. D. Mahanti, *Phys. Rev. Lett.* **96**, 056403 (2006).
- [13] J. Lee, J. Wu, and J. C. Grossman, *Phys. Rev. Lett.* **104**, 016602 (2010).
- [14] T. E. Humphrey and H. Linke, *Phys. Rev. Lett.* **94**, 096601 (2005).
- [15] X. C. Wang *et al.*, and Y. Xue, *Appl. Phys. Lett.* **98**, 222110 (2011).
- [16] G. P. Meisner *et al.*, *Phys. Rev. Lett.* **80**, 3551 (1998).
- [17] A. F. May, J. P. Fleurial, and G. J. Snyder, *Phys. Rev. B* **78**, 125205 (2008).
- [18] J. P. Heremans *et al.*, *Science* **321**, 554 (2008).
- [19] L. D. Hicks and M. S. Dresselhaus, *Phys. Rev. B* **47**, 12727 (1993); *Phys. Rev. B* **47**, 16631 (1993).
- [20] Y. M. Lin and M. S. Dresselhaus, *Phys. Rev. B* **68**, 075304 (2003).
- [21] R. R. Heikes, *Pure Appl. Chem.* **7**, 407 (1963).
- [22] S. Bar-ad, B. Fisher, J. Ashkenazi, and J. Genossar, *Physica C* **156**, 741 (1988).
- [23] See EPAPS Document for supplementary information. For more information on EPAPS, see <http://www.aip.org/pubservs/epaps.html>.
- [ 24 ] If we write the delta-shaped TDF as a normalized Gaussian function  $\lim_{W_\alpha \rightarrow 0} \Xi_\alpha(E) \sim W_\alpha^{-1} e^{-E^2/2W_\alpha^2}$  and approximate Eq. (4) to  $\Xi_\alpha(E) \sim N_\alpha(E)\tau_\alpha(E)v_\alpha^2(E)$  [9], one can find that  $\tau_\alpha(E) \sim 1/W_\alpha^2$  is required since  $N_\alpha(E) \sim 1/W_\alpha$  and  $v_\alpha^2(E) \sim W_\alpha^2$ .
- [25] D. P. Spitzer, *J. Phys. Chem. Solids* **31**, 19 (1970).
- [26] *CRC Handbook of Thermoelectrics*, edited by D. M. Rowe (CRC Press, Boca Raton, 1995).
- [27] The carrier MFP varies from a few nanometers to hundreds of nanometers in different materials. J. R. Szczech, J. M. Higgins, and S. Jin, *J. Mater. Chem.* **21**, 4037 (2011).